THE ASTROPHYSICAL JOURNAL, 290:411–423, 1985 March 15

RADIATIVE TRANSFER EQUATION IN SPHERICAL SYMMETRY

A. PERAIAH AND B. A. VARGHESE
Indian Institute of Astrophysics, Bangalore, India
Received 1984 April 26; accepted 1984 October 5

ABSTRACT

We present a numerical solution of the radiative transfer equation in spherically symmetric geometry using integral operators within the framework of the discrete space theory and expressing the specific intensity in terms of the nodal values of the radius-angle mesh. The solution obtained satisfies the following basic tests: (1) the invariance of the specific intensity in a medium in which radiation is neither absorbed nor emitted, (2) the continuity of the solution in both angle and radial distribution, (3) a numerical proof showing the uniqueness of the solution, and (4) the condition of zero net flux in a scattering medium with one boundary having a specular reflector, and global conservation of energy. The solution is found to satisfy the above tests to the machine accuracy.

Subject heading: radiative transfer

I. INTRODUCTION

There are several approaches to solve the problems of radiative transfer in spherically symmetric media (see, e.g., Hummer and Rybicki 1971; Schmid-Burgk 1973, 1974; Peraiah and Grant 1973; Kalkofen and Wehrse 1984). However, each method has been developed to suit a particular aspect of the problem in question. Most of them involve iteration and are consequently time-consuming. The techniques developed in the framework of discrete space theory (Grant and Hunt 1969*a*, *b*) give direct solutions which are highly accurate. These methods can easily be analyzed numerically, and their physical interpretation is straightforward, at each step of the calculation. However, one has to choose the integration grid in such a way that the solution thus obtained is unique and satisfies the conditions of continuity and stability. Peraiah and Grant (1973) developed such a numerical solution which satisfies the above criteria.

However, the above criteria are satisfied only when we consider a radius-angle grid whose dimensions are small. In an optically thick medium, the process of obtaining the solution becomes time-consuming. Moreover, this particular grid gives unacceptable errors when the solution is sought in the media which neither emit nor absorb radiation. We must obtain a solution which is free from the above defects. Such a solution has been developed in this paper, following the lines of Lathrop and Carlson (1967, 1971). The following steps are taken in obtaining the solution:

1. The specific intensity is expressed in terms of an interpolation formula with the coefficients expressed in terms of the nodal values of the radius-angle grid.
2. The transfer equation is written in terms of this interpolation formula.
3. The integration is performed over the radius-angle grid.

The solution thus obtained is subject to certain basic principles of physics such as the invariance of the specific intensity in vacuum, flux conservation, and so on. Therefore, we did not find it necessary to compare our results with those obtained by other methods. We describe the method of obtaining the solution in § II, and its discussion is given in § III.

II. INTEGRATION OF EQUATION OF TRANSFER OVER THE RADIUS-ANGLE MESH

The time-independent equation of radiative transfer in spherically symmetric geometry is given by

$$\mu \frac{\partial I(r, \mu)}{\partial r} + \frac{1-\mu^2}{r} \frac{\partial I(r, \mu)}{\partial \mu} = K(r)[s(r, \mu) - I(r, \mu)] , \quad (1)$$

and for the oppositely directed beam

$$-\mu \frac{\partial I(r, -\mu)}{\partial r} - \frac{1-\mu^2}{r} \frac{\partial I(r, -\mu)}{\partial \mu} = K(r)[s(r, -\mu) - I(r, -\mu)] . \quad (2)$$

Here $\mu \in (0, 1)$ is the cosine of the angle between the normal to the shells and the ray whose specific intensity is $I(r, \mu)$ at radius r; $K(r)$ is the absorption coefficient and $s(r, \mu)$ is the source function which is given by

$$s(r, \mu) = [1 - \varpi(r)]b(r, \mu) + \tfrac{1}{2}\varpi(r) \int_{-1}^{+1} P(r, \mu, \mu')I(r, \mu)d\mu' , \quad (3)$$

where $\varpi(r)$ is the albedo for single scattering, $b(r, \mu)$ is the Planck function, and $P(r, \mu, \mu')$ is the phase function. In this paper, we consider isotropic scattering, and hence $\varpi(r)$ is set equal to 1.

We shall write that

$$U(r, \mu) = 4\pi r^2 I(r, \mu) , \qquad S(r, \mu) = 4\pi r^2 s(r, \mu) , \qquad B(r, \mu) = 4\pi r^2 b(r, \mu) . \quad (4)$$

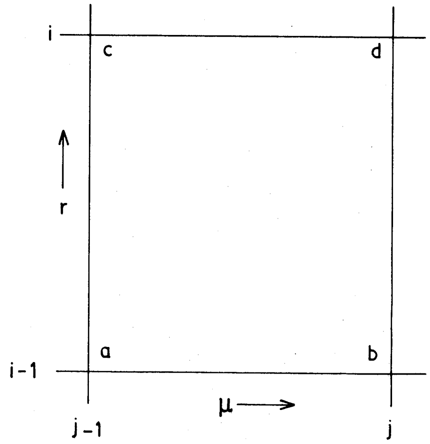

FIG. 1.—Schematic diagram of the angle-radius grid

Substituting equation (4) into equations (1) and (2), we obtain

$$\mu \frac{\partial U(r, \mu)}{\partial r} + \frac{1}{r}\frac{\partial}{\partial \mu}[(1-\mu^2)U(r, \mu)] = K(r)[S(r, \mu) - U(r, \mu)] , \tag{5}$$

$$-\mu \frac{\partial U(r, -\mu)}{\partial r} - \frac{1}{r}\frac{\partial}{\partial \mu}[(1-\mu^2)U(r, -\mu)] = K(r)[S(r, -\mu) - U(r, -\mu)] . \tag{6}$$

Although we have assumed an angle-dependent source term, it is set equal to zero in this paper. However, when we study the polychromatic case with velocities, the angle dependence of the source function becomes important. Equations (5) and (6) are integrated over the radius-angle mesh bounded by $(r_i, r_{i-1}) \times (\mu_j, \mu_{j-1})$ as shown in Figure 1 (see Lathrop and Carlson 1967, 1971).

The specific intensity is expressed by an interpolation formula given by

$$U(r, \mu) \approx (U_{00} + U_{01}\xi) + (U_{10} + U_{11}\xi)\eta , \tag{7}$$

where

$$\xi = \frac{r - \bar{r}}{\Delta r/2} , \qquad \eta = \frac{\mu - \bar{\mu}}{\Delta\mu/2} , \tag{8}$$

$$\bar{r} = \frac{1}{2}(r_i + r_{r-1}) , \qquad \bar{\mu} = \tfrac{1}{2}(\mu_j + \mu_{j-1}) , \tag{9}$$

$$\Delta r = (r_i - r_{i-1}) , \qquad \Delta\mu = (\mu_j - \mu_{j-1}) . \tag{10}$$

We estimate the nodal values of the intensities in terms of the interpolation coefficient U_{00}, U_{01}, U_{10}, and U_{11} (see Fig. 1).

These are given by

$$\begin{aligned} U(r_i, \mu_j) &= U_{00} + U_{01} + U_{10} + U_{11} = U_d , \\ U(r_{i-1}, \mu_j) &= U_{00} - U_{01} + U_{10} - U_{11} = U_b , \\ U(r_i, \mu_{j-1}) &= U_{00} + U_{01} - U_{10} - U_{11} = U_c , \\ U(r_{i-1}, \mu_{j-1}) &= U_{00} - U_{01} - U_{10} + U_{11} = U_a . \end{aligned} \tag{11}$$

From equation (11) we obtain the interpolation coefficients:

$$\begin{aligned} U_{00} &= \tfrac{1}{4}(+U_a + U_b + U_c + U_d) , \\ U_{01} &= \tfrac{1}{4}(-U_a - U_b + U_c + U_d) , \\ U_{10} &= \tfrac{1}{4}(-U_a + U_b - U_c + U_d) , \\ U_{11} &= \tfrac{1}{4}(+U_a - U_b - U_c + U_d) . \end{aligned} \tag{12}$$

We define the operators X and Y such that

$$X = \frac{1}{\Delta\mu}\int_{\Delta\mu} \cdots \, d\mu \,, \tag{13}$$

$$Y = \frac{1}{V}\int_{\Delta r} \cdots \, 4\pi r^2 dr \,. \tag{14}$$

where

$$V = \frac{4\pi}{3}(r_i^3 - r_{i-1}^3) \,. \tag{15}$$

Substituting equation (7) in equation (5), we obtain

$$\frac{2\mu}{\Delta r}(U_{01} + U_{11}\eta) + \frac{1-\mu^2}{r}\frac{2}{\Delta\mu}(U_{10} + U_{11}\xi) - \frac{2\mu}{r}(U_{00} + U_{01}\xi + U_{10}\eta + U_{11}\xi\eta)$$
$$= K(r)[S(r, \mu) - U_{00} - U_{01}\xi - U_{10}\eta - U_{11}\xi\eta] \,. \tag{16}$$

The quantity $S(r, \mu)$ is also expressed by an interpolation formula similar to that given in equation (7). We can write

$$S(r, \mu) = S_{00} + S_{01}\xi + S_{10}\eta + S_{11}\xi\eta \,. \tag{17}$$

The interpolation coefficients S_{00}, S_{01}, S_{10}, and S_{11} are obtained by expressions analogous to equation (12). We apply the operator X to equation (16) and obtain

$$\frac{2}{\Delta r}\left(\bar{\mu}U_{01} + \frac{1}{6}\Delta\mu U_{11}\right) + \frac{2}{r}\frac{1}{\Delta\mu}(1 - \overline{\mu^2})(U_{10} + \xi U_{11}) - \frac{2\bar{\mu}}{r}(U_{00} + U_{01}\xi) - \frac{\Delta\mu}{3r}(U_{10} + U_{11}\xi) = K(r)(S_{00} + S_{01}\xi - U_{00} - U_{01}\xi) \,, \tag{18}$$

where

$$\overline{\mu^2} = (\bar{\mu})^2 + \frac{(\Delta\mu)^2}{12} \,. \tag{19}$$

We now apply the operator Y on equation (18) and obtain

$$\frac{2}{\Delta r}\left(\bar{\mu}U_{01} + \frac{1}{6}\Delta\mu U_{11}\right) + \frac{2}{\Delta\mu}\frac{1-\overline{\mu^2}}{\Delta r}\frac{1}{2}\frac{\Delta A}{\bar{A}}\left(U_{10} + \frac{1}{6}\frac{\Delta r}{\bar{r}}U_{11}\right)$$
$$- \bar{\mu}U_{00}\frac{\Delta A}{V} + \frac{2\bar{\mu}U_{01}}{\Delta r}\left(\bar{r}\frac{\Delta A}{V} - 2\right) - \frac{1}{6}\Delta\mu U_{10}\frac{\Delta A}{V} + \frac{1}{3}\frac{\Delta\mu}{\Delta r}U_{11}\left(\bar{r}\frac{\Delta A}{V} - 2\right)$$
$$= K(r)\left(S_{00} + \frac{1}{6}\frac{\Delta A}{\bar{A}}S_{01} - U_{00} - \frac{1}{6}\frac{\Delta A}{\bar{A}}U_{01}\right), \tag{20}$$

where

$$\bar{A} = \frac{V}{\Delta r} \,, \tag{21}$$

$$\Delta A = 4\pi(r_i^2 - r_{i-1}^2) \,. \tag{22}$$

The interpolation coefficients U_{00}, U_{01}, U_{10}, U_{11} and S_{00}, S_{01} which appear in equation (20) are replaced by their corresponding nodal values U_a, U_b, U_c, and U_d and S_a, S_b, S_c, and S_d (see eq. [12]). Thus, we have

$$\left[\mu_{j-1/2}^{-}(1 + p) + \frac{1}{2}\tau\left(1 + \frac{1}{6}\frac{\Delta A}{\bar{A}}\right) - \frac{1}{2}\frac{1-\overline{\mu^2}}{\Delta\mu}\frac{\Delta A}{\bar{A}}\left(1 + \frac{1}{6}\frac{\Delta r}{\bar{r}}\right)\right]U_c$$
$$+ \left[\mu_{j-1/2}^{+}(1 + p) + \frac{1}{2}\tau\left(1 + \frac{1}{6}\frac{\Delta A}{\bar{A}}\right) + \frac{1}{2}\frac{1-\overline{\mu^2}}{\Delta\mu}\frac{\Delta A}{\bar{A}}\left(1 + \frac{1}{6}\frac{\Delta r}{\bar{r}}\right)\right]U_d$$
$$- \left[\mu_{j-1/2}^{-}(1 + q) - \frac{1}{2}\tau\left(1 - \frac{1}{6}\frac{\Delta A}{\bar{A}}\right) + \frac{1}{2}\frac{1-\overline{\mu^2}}{\Delta\mu}\frac{\Delta A}{\bar{A}}\left(1 - \frac{1}{6}\frac{\Delta r}{\bar{r}}\right)\right]U_a$$
$$- \left[\mu_{j-1/2}^{+}(1 + q) - \frac{1}{2}\tau\left(1 - \frac{1}{6}\frac{\Delta A}{\bar{A}}\right) - \frac{1}{2}\frac{1-\overline{\mu^2}}{\Delta\mu}\frac{\Delta A}{\bar{A}}\left(1 - \frac{1}{6}\frac{\Delta r}{\bar{r}}\right)\right]U_b$$
$$= \frac{1}{2}\tau\left[\left(1 - \frac{1}{6}\frac{\Delta A}{\bar{A}}\right)(S_a + S_b) + \left(1 + \frac{1}{6}\frac{\Delta A}{\bar{A}}\right)(S_c + S_d)\right]. \tag{23}$$

Equation (6) is integrated in a similar way and is written as

$$-\left[\mu_{j-1/2}^{-}(1-p)-\frac{1}{2}\tau\left(1+\frac{1}{6}\frac{\Delta A}{\bar{A}}\right)-\frac{1}{2}\frac{1-\overline{\mu^2}}{\Delta\mu}\frac{\Delta A}{\bar{A}}\left(1+\frac{1}{6}\frac{\Delta r}{\bar{r}}\right)\right]U_c$$

$$-\left[\mu_{j-1/2}^{+}(1-p)-\frac{1}{2}\tau\left(1+\frac{1}{6}\frac{\Delta A}{\bar{A}}\right)+\frac{1}{2}\frac{1-\overline{\mu^2}}{\Delta\mu}\frac{\Delta A}{\bar{A}}\left(1+\frac{1}{6}\frac{\Delta r}{\bar{r}}\right)\right]U_d$$

$$+\left[\mu_{j-1/2}^{-}(1-q)+\frac{1}{2}\tau\left(1-\frac{1}{6}\frac{\Delta A}{\bar{A}}\right)+\frac{1}{2}\frac{1-\overline{\mu^2}}{\Delta\mu}\frac{\Delta A}{\bar{A}}\left(1-\frac{1}{6}\frac{\Delta r}{\bar{r}}\right)\right]U_a$$

$$+\left[\mu_{j-1/2}^{+}(1-q)+\frac{1}{2}\tau\left(1-\frac{1}{6}\frac{\Delta A}{\bar{A}}\right)-\frac{1}{2}\frac{1-\overline{\mu^2}}{\Delta\mu}\frac{\Delta A}{\bar{A}}\left(1-\frac{1}{6}\frac{\Delta r}{\bar{r}}\right)\right]U_b$$

$$=\frac{1}{2}\tau\left[\left(1-\frac{\Delta A}{\bar{A}}\right)(S_a+S_b)+\left(1+\frac{\Delta A}{\bar{A}}\right)(S_c+S_d)\right], \quad (24)$$

where

$$\tau = K.\Delta r\,, \quad (25)$$

$$\mu_{j-1/2}^{+}=\bar{\mu}\left(1+\frac{1}{6}\frac{\Delta\mu}{\bar{\mu}}\right)=\frac{1}{3}(2\mu_j+\mu_{j-1})\,, \quad (26)$$

$$\mu_{j-1/2}^{-}=\bar{\mu}\left(1-\frac{1}{6}\frac{\Delta\mu}{\bar{\mu}}\right)=\frac{1}{3}(\mu_j+2\mu_{j-1})\,, \quad (27)$$

$$p=\frac{\bar{r}}{\Delta r}\frac{\Delta A}{\bar{A}}-\frac{1}{2}\frac{\Delta A}{\bar{A}}-2\,, \quad (28)$$

$$q=2-\frac{1}{2}\frac{\Delta A}{\bar{A}}-\frac{\bar{r}}{\Delta r}\frac{\Delta A}{\bar{A}}\,, \quad (29)$$

Define

$$t=\frac{\Delta r}{\bar{r}}=(r_i-r_{i-1})\Big/\frac{1}{2}(r_i+r_{i-1})\,, \quad (30)$$

and if $t \ll 1$, then

$$\frac{\Delta A}{\bar{A}}=2t\Big/\left(1+\frac{1}{12}t^2\right)\approx 2t\,, \quad (31)$$

$$1\pm\frac{1}{6}\frac{\Delta A}{\bar{A}}=\left(1\pm\frac{1}{3}t+\frac{1}{12}t^2\right)\Big/\left(1\pm\frac{1}{12}t^2\right)\approx 1\pm\frac{1}{3}t\,, \quad (32)$$

and

$$p\approx q\approx -t\,. \quad (33)$$

We write U_a, U_b, U_c, and U_d and S_a, S_b, S_c, and S_d as U_{j-1}^{i-1}, U_j^{i-1}, U_{j-1}^{i}, and U_j^i and S_{j-1}^{i-1}, S_j^{i-1}, S_{j-1}^{i}, and S_j^i, respectively. Equations (23) and (24) can be written as

$$[\mu_{j-1/2}^{-}(1+p)-\rho_{j-1/2}^{i-1/2,+}+\tfrac{1}{2}\tau_{i-1/2}^{+}]U_{j-1}^{i,+}+[\mu_{j-1/2}^{+}(1+p)+\rho_{j-1/2}^{i-1/2,+}+\tfrac{1}{2}\tau_{i-1/2}^{+}]U_j^{i,+}$$
$$-[\mu_{j-1/2}^{-}(1+q)+\rho_{j-1/2}^{i-1/2,-}-\tfrac{1}{2}\tau_{i-1/2}^{-}]U_{j-1}^{i-1,+}-[\mu_{j-1/2}^{+}(1+q)-\rho_{j-1/2}^{i-1/2,-}-\tfrac{1}{2}\tau_{i-1/2}^{-}]U_j^{i-1,+}$$
$$=\tfrac{1}{2}\tau_{i-1/2}^{-}(S_{j-1}^{i-1,+}+S_j^{i-1,+})+\tfrac{1}{2}\tau_{i-1/2}^{+}(S_{j-1}^{i,+}+S_j^{i,+})\,, \quad (34)$$

and

$$[\mu_{j-1/2}^{-}(1+p)-\rho_{j-1/2}^{i-1/2,+}+\tfrac{1}{2}\tau_{i-1/2}^{+}]U_{j-1}^{i,+}+[\mu_{j-1/2}^{+}(1+p)+\rho_{j-1/2}^{i-1/2,+}+\tfrac{1}{2}\tau_{i-1/2}^{+}]U_j^{i,+}$$
$$-[\mu_{j-1/2}^{-}(1+q)+\rho_{j-1/2}^{i-1/2,-}-\tfrac{1}{2}\tau_{i-1/2}^{-}]U_{j-1}^{i-1,+}-[\mu_{j-1/2}^{+}(1+q)-\rho_{j-1/2}^{i-1/2,-}-\tfrac{1}{2}\tau_{i-1/2}^{-}]U_j^{i-1,+}$$
$$=\tfrac{1}{2}\tau_{i-1/2}^{-}(S_{j-1}^{i-1,-}+S_j^{i-1,-})+\tfrac{1}{2}\tau_{i-1/2}^{+}(S_{j-1}^{i,-}+S_j^{i,-})\,, \quad (35)$$

where

$$\tau_{i-1/2}^{+}=\tau_{i-1/2}\left(1+\frac{1}{6}\frac{\Delta A}{\bar{A}}\right)=\tau_{i-1/2}\frac{3r_i^2+2r_ir_{i-1}+r_{i-1}^2}{2(r_i^2+r_ir_{i-1}+r_{i-1}^2)}\,, \quad (36)$$

$$\tau_{i-1/2}^{-} = \tau_{i-1/2}\left(1 - \frac{1}{6}\frac{\Delta A}{\bar{A}}\right) = \tau_{i-1/2}\frac{r_i^2 + 2r_i r_{i-1} + 3r_{i-1}^2}{2(r_i^2 + r_i r_{i-1} + r_{i-1}^2)}, \tag{37}$$

$$\rho_{j-1/2}^{i-1/2,\pm} = \rho_{j-1/2}^{i-1/2}\left(1 \pm \frac{1}{6}\frac{\Delta r}{\bar{r}}\right), \tag{38}$$

$$\rho_{j-1/2}^{i-1/2} = \frac{1}{2}\frac{1-\overline{\mu^2}}{\Delta\mu}\frac{\Delta A}{\bar{A}} = \left[\frac{1 - 1/3(\mu_j^2 + \mu_j\mu_{j-1} + \mu_{j-1}^2)}{2(\mu_j - \mu_{j-1})}\right]\left[\frac{3(r_i^2 - r_{i-1}^2)}{(r_i^2 + r_i r_{i-1} + r_{i-1}^2)}\right]. \tag{39}$$

The source terms $S^{\pm}$ are given by

$$S^{i,+} = (1 - \varpi_i)B^{i,+} + \tfrac{1}{2}\varpi_i(p_i^{++}CU^{i,+} + p_i^{+-}CU^{i,-}), \tag{40}$$

$$S^{i-1,+} = (1 - \varpi_{i-1})B^{i-1,+} + \tfrac{1}{2}\varpi_{i-1}(p_{i-1}^{++}CU^{i-1,+} + p_{i-1}^{+-}CU^{i-1,-}), \tag{41}$$

where the C's are angle quadrature weights. The phase function elements p^{++}, p^{--} are given by

$$p_i^{++} = p(r_i, +\mu_j, +\mu_j), \quad p_i^{+-} = p(r_i, +\mu_j, -\mu_j). \tag{42}$$

The quantities $S^{i,-}$ and $S^{i-1,-}$ are similarly defined.

In a stationary medium we have

$$B^{i,+} = B^{i,-}, \quad B^{i-1,+} = B^{i-1,-}, \tag{43}$$

and, furthermore,

$$U^{i,\pm} = U(r_i, \pm\mu_j). \tag{44}$$

The interval $\mu \in (0, 1)$ is partitioned into $\mu_0 < \mu_1 < \mu_2 < \mu_3 \cdots < \mu_J = 1$. We also need equation at $j = J$. This can be obtained by putting $\rho = 0$ and $\mu_J^+ = \mu_J^- = 1$. Thus,

$$(\mu_J + \tfrac{1}{2}\tau_{i-1/2}^{+})U_J^{i,+} - (\mu_J - \tfrac{1}{2}\tau_{i-1/2}^{-})U_J^{i-1} = \tfrac{1}{2}\tau_{i-1/2}^{-}S_J^{i-1,+} + \tfrac{1}{2}\tau_{i-1/2}^{+}S_J^{i,+}, \tag{45}$$

and

$$-(\mu_J - \tfrac{1}{2}\tau_{i-1/2}^{+})U_J^{i,-} + (\mu_J + \tfrac{1}{2}\tau_{i-1/2}^{-})U_J^{i-1,-} = \tfrac{1}{2}\tau_{i-1/2}^{-}S_J^{i-1,-} + \tfrac{1}{2}\tau_{i-1/2}^{+}S_J^{i,-}. \tag{46}$$

Here $\rho = 0$ (see eq. [39]).

Now equations (34), (35), (45), and (46) can be succinctly written for J angles. We omit the subscript $i - \frac{1}{2}$ for simplicitly. We thus have

$$\left[\boldsymbol{M}_p^+ - \boldsymbol{\rho}^+ + \tfrac{1}{2}\tau^+\boldsymbol{Q}(\boldsymbol{I} - \gamma^{++})\right]\boldsymbol{U}_i^+ - [\boldsymbol{M}_q^+ + \boldsymbol{\rho}^- - \tfrac{1}{2}\tau^-\boldsymbol{Q}(\boldsymbol{I} - \gamma^{++})]\boldsymbol{U}_{i-1}^+ = (1-\varpi)\tau\boldsymbol{Q}\boldsymbol{B}^+ + \tfrac{1}{2}\tau^+\boldsymbol{Q}\gamma^{+-}\boldsymbol{U}_{i-1}^- + \tfrac{1}{2}\tau^-\boldsymbol{Q}\gamma^{+-}\boldsymbol{U}_i^-, \tag{47}$$

and

$$-[\boldsymbol{M}_p^- - \boldsymbol{\rho}^+ - \tfrac{1}{2}\tau^+\boldsymbol{Q}(\boldsymbol{I} - \gamma^{--})]\boldsymbol{U}_i^- + [\boldsymbol{M}_q^- + \boldsymbol{\rho}^- + \tfrac{1}{2}\tau^-\boldsymbol{Q}(\boldsymbol{I} - \gamma^{--})]\boldsymbol{U}_{i-1}^- = (1-\varpi)\tau\boldsymbol{Q}\boldsymbol{B}^- + \tfrac{1}{2}\tau^+\boldsymbol{Q}\gamma^{-+}\boldsymbol{U}_i^+ + \tfrac{1}{2}\tau^-\boldsymbol{Q}\gamma^{-+}\boldsymbol{U}_i^+, \tag{48}$$

where

$$\boldsymbol{M}_p^+ = (1+p)\boldsymbol{M}, \quad \boldsymbol{M}_p^- = (1-p)\boldsymbol{M}, \quad \boldsymbol{M}_q^+ = (1+q)\boldsymbol{M}, \quad \boldsymbol{M}_q^- = (1-q)\boldsymbol{M}, \tag{49}$$

$$\boldsymbol{M} = \begin{bmatrix} \mu_{1/2}^- & \mu_{1/2}^+ & & & \\ & \mu_{3/2}^- & \ddots & \mu_{3/2}^+ & \ddots \\ & & & \mu_{j-1/2}^- & \mu_{j-1/2}^+ \\ & & & & \mu_J \end{bmatrix} \tag{50}$$

$$\boldsymbol{\rho}^{\pm} = \begin{bmatrix} \rho_{1/2}^{\pm} & -\rho_{1/2}^{\pm} & & & \\ & \rho_{3/2}^{\pm} & \ddots & -\rho_{3/2}^{\pm} & \ddots \\ & & & \rho_{j-1/2}^{\pm} & -\rho_{j-1/2}^{\pm} \\ & & & & 0 \end{bmatrix} \tag{51}$$

$$\boldsymbol{Q} = \begin{bmatrix} 1 & 1 & & & \\ & 1 & \ddots & 1 & \ddots \\ & & & 1 & 1 \\ & & & & 1 \end{bmatrix} \tag{52}$$

$$\gamma^{++} = \tfrac{1}{2}\varpi \boldsymbol{P}^{++}\boldsymbol{C}\,, \quad \gamma^{--} = \tfrac{1}{2}\varpi \boldsymbol{P}^{--}\boldsymbol{C}\,, \quad \gamma^{+-} = \tfrac{1}{2}\varpi \boldsymbol{P}^{+-}\boldsymbol{C}\,, \quad \gamma^{-+} = \tfrac{1}{2}\varpi \boldsymbol{P}^{-+}\boldsymbol{C}\,, \tag{53}$$

and $\boldsymbol{I}$ is the identity matrix.

Let us introduce the following:

$$\bar{\rho}_{\pm} = \boldsymbol{Q}^{-1}\rho^{\pm}\,, \quad \boldsymbol{M}_1 = \boldsymbol{Q}^{-1}\boldsymbol{M}_p^+\,, \quad \boldsymbol{M}_2 = \boldsymbol{Q}^{-1}\boldsymbol{M}_p^-\,, \quad \boldsymbol{M}_3 = \boldsymbol{Q}^{-1}\boldsymbol{M}_q^+\,, \quad \boldsymbol{M}_4 = \boldsymbol{Q}^{-1}\boldsymbol{M}_q^-\,,$$

and rewrite equations (47) and (48) as follows:

$$[\boldsymbol{M}_1 - \bar{\rho}_+ + \tfrac{1}{2}\tau^+(\boldsymbol{I} - \gamma^{++})]\boldsymbol{U}_i^+ - [\boldsymbol{M}_3 + \bar{\rho}_- - \tfrac{1}{2}\tau^-(\boldsymbol{I} - \gamma^{++})]\boldsymbol{U}_{i-1}^+ = \tau(1-\varpi)\boldsymbol{B}^+ + \tfrac{1}{2}\tau^-\gamma^{+-}\boldsymbol{U}_{i-1}^- + \tfrac{1}{2}\tau^+\gamma^{+-}\boldsymbol{U}_i^-\,, \tag{55}$$

and

$$-[\boldsymbol{M}_2 - \bar{\rho}_+ - \tfrac{1}{2}\tau^+(\boldsymbol{I} - \gamma^{--})]\boldsymbol{U}_i^- + [\boldsymbol{M}_4 + \bar{\rho}_- + \tfrac{1}{2}\tau^-(\boldsymbol{I} - \gamma^{--})]\boldsymbol{U}_{i-1}^- = \tau(1-\varpi)\boldsymbol{B}^- + \tfrac{1}{2}\tau^-\gamma^{-+}\boldsymbol{U}_{i-1}^+ + \tfrac{1}{2}\tau^+\gamma^{-+}\boldsymbol{U}_i^+\,. \tag{56}$$

If we assume that U_{i-1}^+ and U_i^- are the intensities of the incident radiation and U_i^+ and U_{i-1}^- are the output intensities, then equations (55) and (56) can be written as

$$\begin{bmatrix} \boldsymbol{U}_i^+ \\ \boldsymbol{U}_{i-1}^- \end{bmatrix} = \boldsymbol{K}^{-1}\begin{bmatrix} \boldsymbol{X}_1 & \boldsymbol{X}_2 \\ \boldsymbol{X}_3 & \boldsymbol{X}_4 \end{bmatrix}\begin{bmatrix} \boldsymbol{U}_{i-1}^+ \\ \boldsymbol{U}_i^- \end{bmatrix} + \boldsymbol{K}^{-1}\tau(1-\varpi)\begin{bmatrix} \boldsymbol{B}^+ \\ \boldsymbol{B}^- \end{bmatrix}, \tag{57}$$

where

$$\boldsymbol{X}_1 = \boldsymbol{M}_3 + \bar{\rho}_- - \tfrac{1}{2}\tau^-(\boldsymbol{I} - \gamma^{++})\,, \quad \boldsymbol{X}_2 = \tfrac{1}{2}\tau^+\gamma^{+-}\,, \quad \boldsymbol{X}_3 = \tfrac{1}{2}\tau^-\gamma^{-+}\,, \quad \boldsymbol{X}_4 = \boldsymbol{M}_2 - \bar{\rho}_+ - \tfrac{1}{2}\tau^+(\boldsymbol{I} - \gamma^{--})\,,$$

and

$$\boldsymbol{K} = \begin{bmatrix} \boldsymbol{Y}_1 & \boldsymbol{Y}_2 \\ \boldsymbol{Y}_3 & \boldsymbol{Y}_4 \end{bmatrix}, \tag{58}$$

where

$$\boldsymbol{Y}_1 = \boldsymbol{M}_1 - \bar{\rho}_+ + \tfrac{1}{2}\tau^+(\boldsymbol{I} - \gamma^{++})\,, \quad \boldsymbol{Y}_2 = -\tfrac{1}{2}\tau^-\gamma^{+-}\,, \quad \boldsymbol{Y}_3 = -\tfrac{1}{2}\tau^+\gamma^{-+}\,, \quad \boldsymbol{Y}_4 = \boldsymbol{M}_4 + \bar{\rho}_- + \tfrac{1}{2}\tau^-(\boldsymbol{I} - \gamma^{--})\,.$$

We can compare equation (57) with the interaction principle (see Preisendorfer 1965; Grant and Hunt 1969*a*; Peraiah 1984) given by

$$\begin{bmatrix} \boldsymbol{U}_i^+ \\ \boldsymbol{U}_{i-1}^- \end{bmatrix} = \begin{bmatrix} \boldsymbol{t}(i, i-1) & \boldsymbol{r}(i-1, i) \\ \boldsymbol{r}(i, i-1) & \boldsymbol{t}(i-1, i) \end{bmatrix}\begin{bmatrix} \boldsymbol{U}_{i-1}^+ \\ \boldsymbol{U}_i^- \end{bmatrix} + \begin{bmatrix} \boldsymbol{\Sigma}_{i-1/2}^+ \\ \boldsymbol{\Sigma}_{i-1/2}^- \end{bmatrix}, \tag{59}$$

where $\boldsymbol{t}(i, i-1)$, $\boldsymbol{t}(i-1, i)$, $\boldsymbol{r}(i, i-1)$, and $\boldsymbol{r}(i-1, i)$ are the transmission and reflection operators which interact with the incident radiation given by the intensities $\boldsymbol{U}_{i-1}^+$ and $\boldsymbol{U}_i^-$, giving rise to the output intensities $\boldsymbol{U}_i^+$ and $\boldsymbol{U}_{i-1}^-$ which include the contribution from the internal sources $\boldsymbol{\Sigma}_{i-1/2}^+$ and $\boldsymbol{\Sigma}_{i-1/2}^-$. By direct comparison of equations (57) and (59), we obtain the transmission and reflection operators, $\boldsymbol{t}(i, i-1)$, $\boldsymbol{t}(i-1, i)$, and $\boldsymbol{r}(i-1, i)$. These are given in the Appendix.

The above operators are calculated for a mesh with boundaries $(r_{i-1}, r_i) \times (\mu_{j-1}, \mu_j)$, and the size of the optical depth is determined by the conditions of stability and continuity of the solution. This is called the optical depth in the fundamental shell, or τ_f.

If the optical depth of the atmosphere is larger than the τ_f, then the atmosphere is divided into a number of shells each of which satisfies the conditions of stability. Then, the radiation field in the atmosphere is calculated by using the internal field algorithm (Grant and Hunt 1969*a* or Peraiah and Grant 1973).

For the sake of completeness, we shall quote these formulae from the above references. We divide the atmosphere into N shells for which the r and t operators are calculated (see Fig. 2). We first compute the following operators sequentially for $n = 1, 2, \ldots, N$ ($n = 1$ at $\tau = 0$ or $r = r_{\max}$ or $r = B$; $n = N$ at $\tau = T$ or $r = r_{\min}$ or $r = A$):

$$\begin{aligned} \boldsymbol{r}(1, n+1) &= \boldsymbol{r}(n, n+1) + \boldsymbol{t}(n+1, n)\boldsymbol{r}(1, n)\boldsymbol{T}_{n+1/2}\,\boldsymbol{t}(n, n+1)\,, \\ \boldsymbol{V}_{n+1/2}^+ &= \hat{\boldsymbol{t}}(n+1, n)\boldsymbol{V}_{n-1/2}^+ + \boldsymbol{\Sigma}^+(n+1, n) + \boldsymbol{R}_{n+1/2}\,\boldsymbol{\Sigma}^-(n, n+1)\,, \\ \boldsymbol{V}_{n+1/2}^- &= \hat{\boldsymbol{r}}(r+1, n)\boldsymbol{V}_{n+1/2}^+ + \boldsymbol{T}_{n+1/2}\,\boldsymbol{\Sigma}^-(n, n+1)\,, \end{aligned} \tag{60}$$

with the initial conditions

$$\begin{aligned} \boldsymbol{r}(1, 1) &= 0\,, \\ \boldsymbol{V}_{1/2}^+ &= \boldsymbol{U}^+(B)\,, \end{aligned} \tag{61}$$

where

$$\begin{aligned} \hat{\boldsymbol{t}}(n+1, n) &= \boldsymbol{t}(n+1, n)K_{n+1/2}\,, \\ \hat{\boldsymbol{r}}(n+1, n) &= \boldsymbol{r}(n+1, n)\boldsymbol{K}_{n+1/2}\,, \\ \boldsymbol{R}_{n+1/2} &= \hat{\boldsymbol{t}}(n+1, n)\boldsymbol{r}(1, n)\,, \\ \boldsymbol{T}_{n+1/2} &= [\boldsymbol{I} - \boldsymbol{r}(n+1, n)\boldsymbol{r}(1, n)]^{-1}\,, \\ \boldsymbol{K}_{n+1/2} &= [\boldsymbol{I} - \boldsymbol{r}(1, n)\boldsymbol{r}(n+1, n)]^{-1}\,. \end{aligned} \tag{62}$$

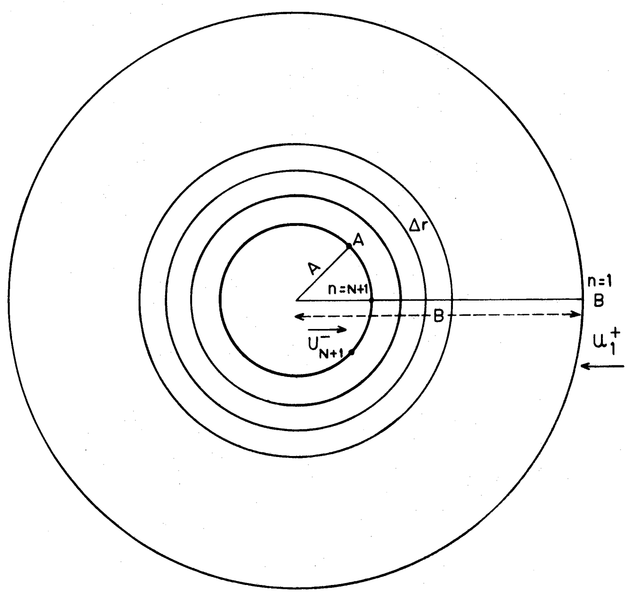

FIG. 2*a*

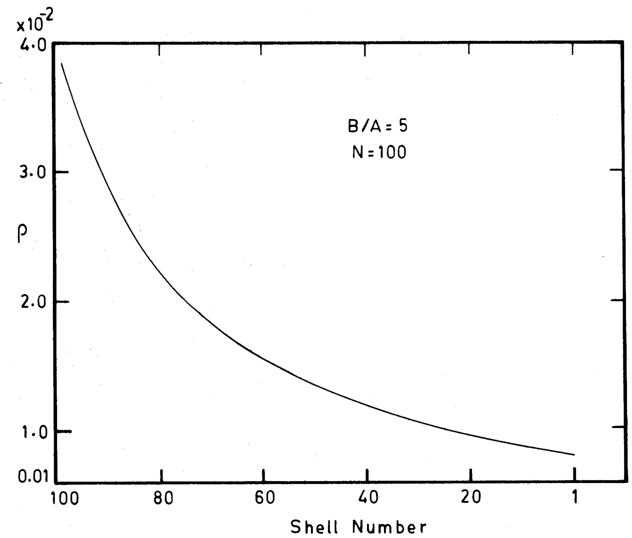

FIG. 2*b*

FIG. 2.—(*a*) Schematic diagram of the spherically symmetric medium. *A* is the inner radius, and *B* is the outer radius of the spherical medium. (*b*) Curvature factor $\rho(=\Delta r/\bar{r})$ is plotted against the shell number. Notice that the curvature factor falls rapidly near the center of the sphere.

Then we compute the intensities at the shell boundaries with the formulae, for $n = N, N-1, N-2, \ldots, 2, 1$, given by

$$\begin{aligned} U^+_{n+1} &= r(1, n+1)U^-_{n+1} + V^+_{n+1/2} , \\ U^-_n &= \hat{t}(n, n+1)U^-_{n+1} + V^-_{n+1/2} , \end{aligned} \tag{63}$$

with the initial condition

$$U^-_{N+1} = U^-(A) , \tag{64}$$

and

$$\hat{t}(n, n+1) = T_{n+1/2}\, t(n, n+1) . \tag{65}$$

If we have a nonemitting reflecting surface at *A* (see Fig. 2) with reflecting operator r_G, then

$$U^-_{N+1} = r_G\, U^+_{N+1} , \tag{66}$$

and equation (63) needs modifying for $n = N$. Thus,

$$U^+_{N+1} = [I - r(1, N+1)]^{-1} V^+_{N+1/2} , \tag{67}$$

from which U^-_{N+1} can be obtained by using equation (66). Then the rest of the intensities can be calculated using equation (63). In the next section we shall describe the results and the tests we apply to the solution developed in this section.

III. TESTS AND DISCUSSION OF THE METHOD

The method described in the previous section must be tested for its stability and accuracy. The solution should also satisfy certain fundamental physical processes. Therefore, we shall test the solution by the following examples:

1) The invariance of the specific intensity in a nonabsorbing and nonemitting medium:

2) Continuity of the solution both in the angle and radial coordinates, verified with Gaussian points as well as trapezoidal points:

3) Uniqueness of the solution:

4) The condition of zero net flux in the case of a specular reflecting boundary at the inner surface in a purely scattering spherical medium and global conservation of flux in such a medium.

The above tests have been performed for various values of the parameters B/A and T, where B and A are the outer and inner radii of the atmosphere and T is the total optical depth of the medium (see Fig. 2). In all these calculations, we assumed an isotropically scattering medium and set $\varpi = 1$. The tests are described below.

a) Invariance of the Specific Intensity

The invariance of the specific intensity is explained clearly in Mihalas (1978). When there are no absorbing or emitting sources, the specific intensity of the radiation field remains constant. It becomes important to check this condition on the solution which is derived in the previous section.

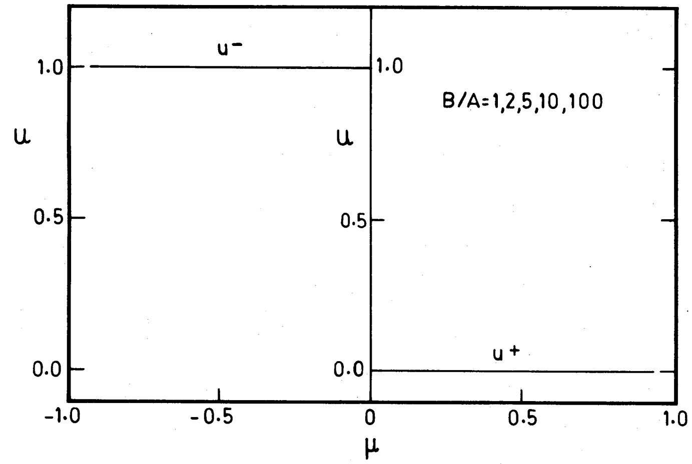

FIG. 3.—Invariance of specific intensity. The angular distribution is given. All the outward intensities (U^-) are always unity [because the incident intensities $U^-_{N+1}(\mu_j) = 1$], and the inward intensities (U^+) are always zero.

It is interesting to see how the term due to the curvature,

$$\frac{1-\mu^2}{r}\frac{\partial I(r, \mu)}{\partial \mu},$$

would behave numerically. For example, if we set $\tau = 0$ in vacuum, the reflection matrices $\boldsymbol{r}(i, i-1)$ and $\boldsymbol{r}(i-1, i)$ vanish, and the transmission matrices become (see Appendix),

$$\boldsymbol{t}(i, i-1) = (\boldsymbol{M}_1 - \bar{\boldsymbol{\rho}}_+)^{-1}(\boldsymbol{M}_3 + \bar{\boldsymbol{\rho}}_-),$$

and

$$\boldsymbol{t}(i-1, i) = (\boldsymbol{M}_4 - \bar{\boldsymbol{\rho}}_-)^{-1}(\boldsymbol{M}_2 - \bar{\boldsymbol{\rho}}_+). \quad (68)$$

When plane-parallel stratification is considered, we immediately see that $\boldsymbol{t}(i, i-1) = \boldsymbol{t}(i-1, i) = \boldsymbol{I}$ (since $\bar{\boldsymbol{\rho}}_+ = \bar{\boldsymbol{\rho}}_- = 0$ and $p = q = 0$, and therefore $\boldsymbol{M}_1 = \boldsymbol{M}_2 = \boldsymbol{M}_3 = \boldsymbol{M}_4$). However, in the case of spherically symmetric media the quantities $\bar{\boldsymbol{\rho}}_+$ and $\bar{\boldsymbol{\rho}}_-$ exist, and the resulting expressions are more complicated.

Therefore we decided to test this case and see whether any numerical error is introduced because of the presence of the terms $\bar{\boldsymbol{\rho}}_+$ and $\bar{\boldsymbol{\rho}}_-$ in the transmission matrices. We considered the following boundary conditions:

$$U^-_{N+1}(\tau = T, \mu_j) = 1 \quad (69)$$

$$U^+_1(\tau = 0, \mu_j) = 0 \quad (70)$$

for all μ_j's.

Equation (69) represents the incident radiation with unit intensity on the atmosphere where the radius is minimum, and equation (70) represents the boundary condition at the maximum radius. Here no radiation is incident on the atmosphere. We have set $B/A = 1, 2, 5, 10, 100$. Different values of B/A will change the curvature factors $\Delta r/\bar{r}$ considerably and affect the numerical errors. Therefore, we divide the spherical shells into smaller shells so that the quantity $\Delta r/\bar{r}$ will not destabilize the numerical solution (see below). The results are presented in Figure 3.

We notice that the outward intensities for all angles are constant and equal to the incident intensities. There is no radiation directed inward. This is true at all radial points for any given B/A. The value of B/A is set equal to 100, and we found that the intensities behave in the same manner as when $B/A = 2$ or 5. It should be mentioned here that the solution developed in Peraiah and Grant (1973) gave rise to negative intensities in vacuum, although the flux is conserved globally to the machine accuracy. In the present method, even when we have chosen a large $\Delta r/\bar{r}$ in the fundamental shell, we have always obtained positive intensities. We thus verify the invariance of the specific intensity in the spherical medium which contains neither sources nor sinks.

b) Continuity of the Solution

We shall show that the numerical solution we developed is continuous both in the angle and radial coordinates. For obtaining continuity, we must have nonnegative matrices of reflection and transmission whose elements are all less than unity (see Grant and Hunt 1969*a*, *b*). This is justified on physical grounds because the sum of transmitted and reflected light should be equal to the total incident radiation. From the equations presented in the Appendix, we see that the quantities $\boldsymbol{\Delta}^+$, $\boldsymbol{\Delta}^-$ in equation (A3) should be positive, so that $t(i, i-1)\, r(i, i-1)$, and so on, should also be positive. If $\boldsymbol{\Delta}^\pm$ are to be positive, we need (see Peraiah and Grant 1973 or Peraiah 1984) the diagonal elements of the matrices $\boldsymbol{\Delta}^+$, $\boldsymbol{\Delta}^-$ to satisfy the condition that

$$[\boldsymbol{M}_1 - \bar{\boldsymbol{\rho}}_+ + \tfrac{1}{2}\tau^+(\boldsymbol{I} - \gamma^{++})]_{jj} \geq 0,$$
$$[\boldsymbol{M}_4 + \bar{\boldsymbol{\rho}}_- + \tfrac{1}{2}\tau^-(\boldsymbol{I} - \gamma^{--})]_{jj} \geq 0, \quad (71)$$

while the off-diagonal elements should satisfy

$$[M_1 - \bar{\rho}_+ + \tfrac{1}{2}\tau^+(I - \gamma^{++})]_{jk} \leq 0 \,,$$
$$[M_4 + \bar{\rho}_- + \tfrac{1}{2}\tau^-(I - \gamma^{--})]_{jk} \leq 0 \,. \tag{72}$$

By expanding equations (71) and (72) we can calculate the critical curvature factor and the optical depth for which nonnegative r and t operators (reflection and transmission operators) can be obtained. This restriction on the optical and geometrical depths which arises in case of stability and continuity of the solution forces us to divide the spherical medium into several fundamental shells. If the optical depth of the medium is very large, we can divide the medium into a small number of shells, each of which is substantially larger than the fundamental one, and use the star product algorithm given in Grant and Hunt (1969*a*) to obtain correct r and t operators.

In an isotropically scattering medium, with phase function $p(r, \mu_j, \mu_k) = 1$, and for Gaussian points with four angles in each quadrant, one obtains maximum optical depth up to 0.5 and the curvature factor $\Delta r/\bar{r}$ less than 10^{-3}. For a given geometrical thickness of the fundamental shell, the curvature factor $\rho = \Delta r/\bar{r}$ increases toward the center of the sphere (see Fig. 2*a*). We have considered a spherical medium with $B/A = 5$ and divided this into 100 shells. The curvature factor is largest at shell number 100 nearest to the center (or at $r = A$) and is minimum at shell number 1 (or at $r = B$). In cases such as given in Figure 2*a*, we make use of the star algorithm because the curvature factor in each shell is greater than 10^{-3}. We have employed the boundary conditions given in equations (69) and (70).

In Figures 4 and 5, we have plotted the angular distribution of the solution for $B/A = 2$, $T = 20$, 50 and $B/A = 5$ and $T = 50$, respectively, where T is the total optical depth. The solution is given at various internal points. We can see that the solution is quite smooth and continuous. We shall show uniqueness latter. The quantities U^+ and U^- represent the intensities directed inward and outward, respectively. In Figure 4, the solid lines represent the solution corresponding to the optical depth 0.02 in the fundamental shell, and the total optical depth is equal to 20. The broken curves correspond to an optical depth 0.05 in the fundamental shell with total optical depth equal to 50. In the deep interior the two curves are graphically unresolvable. In the outer regions the two curves separate out considerably. We see that more radiation is coming outward for $T = 20$ than for $T = 50$. This behavior reverses, although marginally, in the case of the radiation directed inward. Figure 5 gives the same type of results for $B/A = 5$ and $T = 50$. We notice that the intensities in the case of $B/A = 5$, $T = 50$ (Fig. 5) are reduced compared to those in Figure 4 for $B/A = 2$, and $T = 50$.

We considered a medium in which the optical depth varies as $1/r^2$. The total optical depth is taken to be equal to ~ 200, and $B/A = 5$, and the results are presented in Figure 6. Here we have employed the star product algorithm to obtain the r and t operators in an optically thick shell. The results are similar to those presented in Figures 4 and 5. Figures 7 and 8 give the radial distribution of the intensities directed inward (U^+) and intensities (U^-) directed outward. These are plotted against log τ. The four curves in each of the Figures 7 and 8 correspond to the four angles we employed. These are Gaussian quadrature points on $\mu \in (0, 1)$ given by

$$\mu_1 = 0.06943 \,, \quad \mu_2 = 0.33001 \,, \quad \mu_3 = 0.66999 \,, \quad \mu_4 = 0.93057 \tag{73}$$

(see Abramowitz and Stegun 1970).

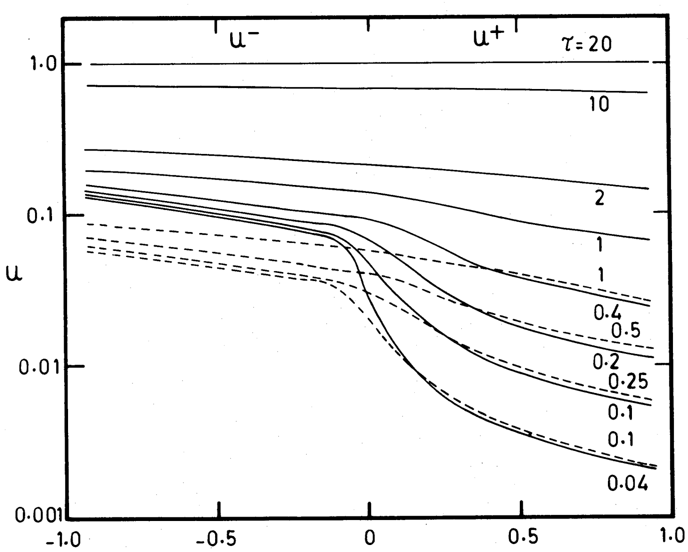

FIG. 4

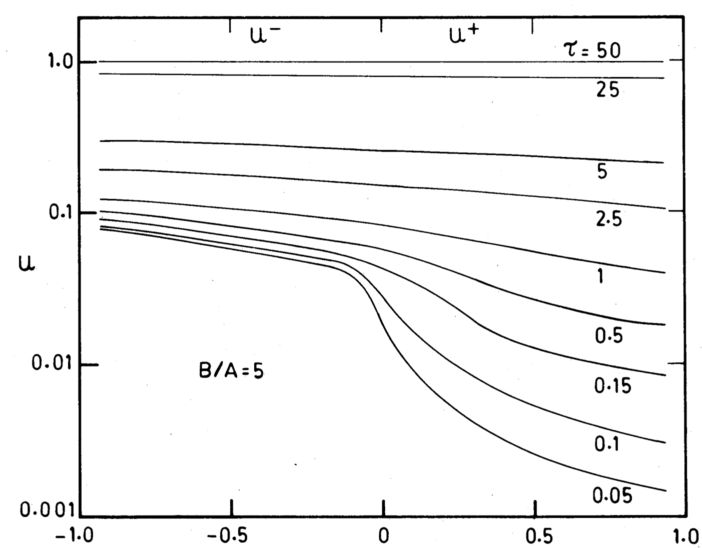

FIG. 5

FIG. 4.—Angular distribution of the intensities for $B/A = 2$. *Dotted lines*, $T = 50$; *solid lines*, $T = 20$

FIG. 5.—Same as Fig. 4, but with $B/A = 5$

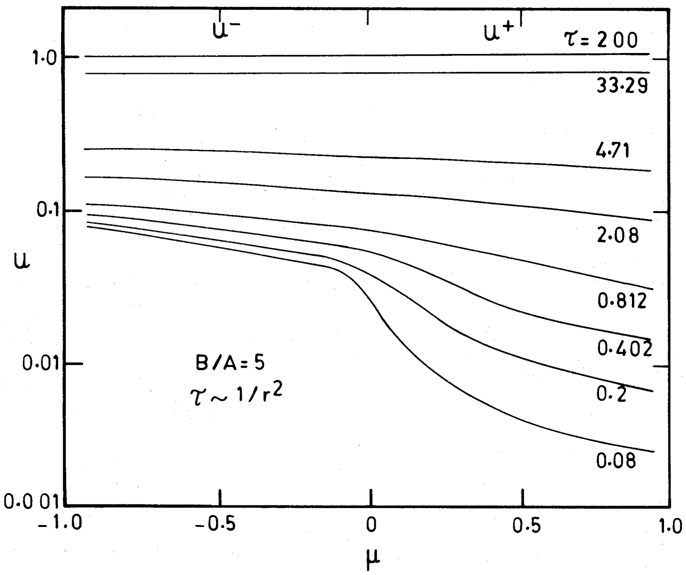

FIG. 6

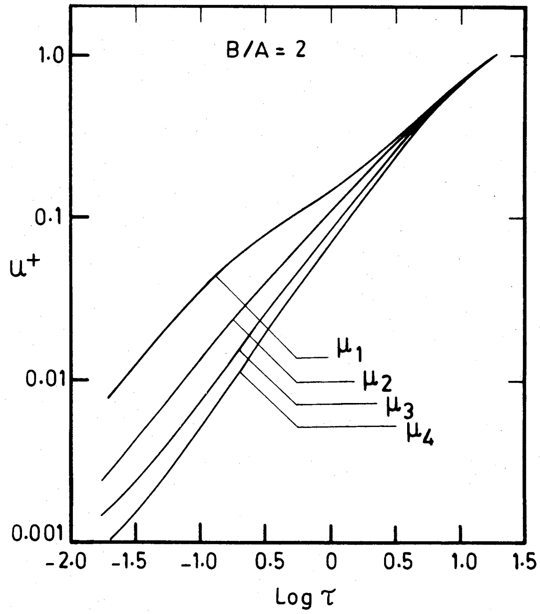

FIG. 7

FIG. 6.—Angular distribution of the intensities for $B/A = 5$. We assumed that the optical depth varies as $1/r^2$.

FIG. 7.—Radial distribution of the intensities directed inward (U^+) for the rays corresponding to μ_1, μ_2, μ_3, and μ_4

We can see clearly from these curves that the radial variation of the intensities is free from numerical instabilities. In the case of radiation directed outward (U^-) the maximum amount of radiation is propagated along the ray with angle $\cos^{-1} \mu_4$ made with the radius vector, while in the case of the beam directed inward the maximum of intensity is propagated by the ray with the angle $\cos^{-1} \mu_1$. In many configurations (such as shell stars, planetary nebulae, and so on) there exists a region which is quite sparse (or almost vacuum) between the star and the shell. It will be interesting to see how the solution behaves in the vacuum and in the outer shell filled with scattering material. We have choosen an atmosphere with $B/A = 2$ in which a shell with no matter exists between the star and the outer layer of the atmosphere, and the geometrical thickness of the shell is set equal to $0.1A$. The optical depth T of the outer shell is taken to be 25. The boundary conditions are the same as those given in equations (69) and (70). The angular distribution is given in Figure 9. The intensities nearest to the vacuum are only slightly different from the incident intensities $[U^-_{N+1}(\mu_j) = 1]$, but the intensities inside the vacuum again maintain the invariance of specific intensity.

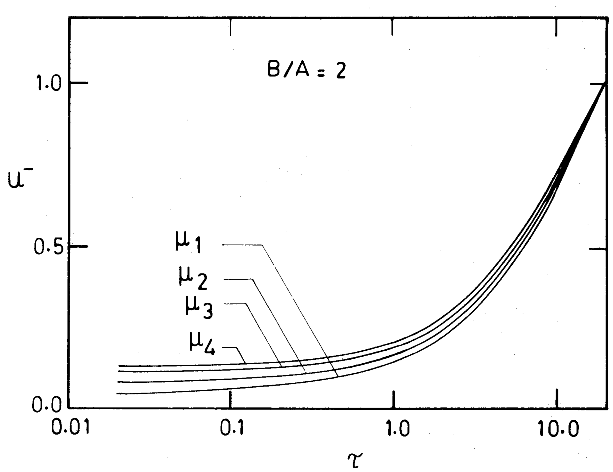

FIG. 8

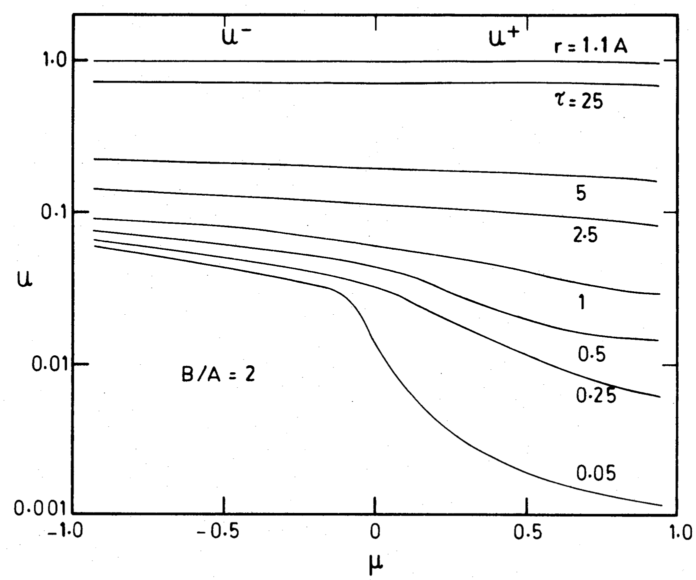

FIG. 9

FIG. 8.—Radial distribution of the intensities directed outward (U^-) for μ_1, μ_2, μ_3, and μ_4

FIG. 9.—Angular distribution of the intensities from a medium which is partly vacuum. The region between A and $0.1A$ is vacuum

TABLE 1

RESULTS OF EQUATION (74)

τ	$U^+(\mu=0)$	$U^-(\mu=0)$	$U^+(\mu=0) - U^-(\mu=0)$
20.0.........	0.999980	1.000000	2.0×10^{-5}
18.0.........	0.886744	0.886745	1.0×10^{-6}
16.0.........	0.800261	0.800247	1.4×10^{-5}
14.0.........	0.712000	0.712008	8.0×10^{-6}
12.0.........	0.621805	0.621808	3.0×10^{-6}
10.0.........	0.529582	0.529585	3.0×10^{-6}
8.0.........	0.435312	0.435314	4.0×10^{-6}
6.0.........	0.338969	0.338960	1.0×10^{-6}
4.0.........	0.240523	0.240527	1.0×10^{-6}
2.0.........	0.139842	0.139843	1.0×10^{-6}
1.0.........	0.088017	0.088014	3.0×10^{-6}
0.8.........	0.079001	0.079006	5.0×10^{-6}
0.6.........	0.067186	0.067185	1.0×10^{-6}
0.4.........	0.056388	0.056379	9.0×10^{-6}
0.2.........	0.045118	0.045118	0.0

There is another important check on the method. For example, at $\mu = 0$ we must have

$$U^+(\mu = 0) \equiv U^-(\mu = 0) . \tag{74}$$

In our calculations, we employed the roots of the Gauss-Legendre polynomial over $\mu \in (0, 1)$ for the angle quadrature, and these points are distributed symmetrically away from $\mu = 0$ (see eq. [73]), but there is no root at $\mu = 0$. However, the trapezoidal points may be set to start at $\mu = 0$. Therefore we can verify equation (74) by employing the trapezoidal points. For this purpose, we considered a spherical medium with $B/A = 1.5$ and $T = 20$. In Table 1, we have listed the values of $U^+(\mu = 0)$ and $U^-(\mu = 0)$ and $|U^+(\mu = 0) - U^-(\mu = 0)|$ at different optical depths in the medium. These calculations have been done with single precision, and we can see that the quantity $|U^+(\mu = 0) - U^-(\mu = 0)|$ is found to be accurate almost to the machine accuracy. We thus have shown that the method gives us a solution which is stable and continuous. We shall prove below the uniqueness of the solution.

c) *Uniqueness of the Solution*

The numerical solution we have obtained should be tested for uniqueness. The uniqueness can be tested both analytically and numerically (see Grant and Hunt 1969*b* for analytical proof). The solution is unique if we can obtain nonnegative r and t operators, and these can be obtained if we calculate them in a shell whose thickness is less than τ_f. We can check uniqueness numerically as follows: divide the fundamental shell into two shells of equal thickness. We then calculate the r and t operators of each of them and add them by the star algorithm. This solution should be identical with that obtained for a single shell with τ_f. In Table 2 we describe the emergent intensities corresponding to μ_1, μ_2, μ_3, and μ_4. The numbers in the first row correspond to the intensities from a single shell with $\tau = \tau_f$, and those in the second row correspond to the emergent intensities from two shells each with $\tau = \frac{1}{2}\tau_f$. It is easily seen that they differ only in the fourth digit which occurs because, in adding the two shells by the star algorithm, we have assumed that the curvature factors in both shells are equal. This is not true because the curvature factor is different for different shells (see Fig. 2*a*). One has to be careful in adding the shells by the star algorithms. The correct curvature factor $\Delta r/\bar{r}$ must be utilized in each shell and not an approximate value of it when the r and t matrices are computed in the fundamental shell. The star addition of such shells yields a solution correct to the accuracy prescribed by the machine. This is however, time-consuming, and if one is willing to sacrifice part of the accuracy, one can use the doubling version of the star algorithm by calculating the r and t operators in a subdivided fundamental shell. In this process, we assume a constant curvature factor in all the fundamental shells. The doubling algorithm will be fast, and one obtains results which are slightly less accurate.

d) *Zero Net Flux: Specular Reflection at the Inner Boundary*

If we consider a perfectly reflecting surface at A (see Fig. 2) and assume a conservatively scattering medium, the radiation that is incident at the surface B will get completely reflected at the surface A, and therefore the net flux at any internal point will be exactly zero. The boundary condition at B is given as

$$U_1^+(\mu_j) = 1 , \tag{75}$$

while the boundary condition at the surface A is governed by equations (66) and (67) with $\boldsymbol{r}_G = \boldsymbol{I}$. The results are given in Table 3.

TABLE 2

CHECK ON UNIQUENESS OF SOLUTION

τ	μ_1	μ_2	μ_3	μ_4
τ_f	0.6890	0.8806	0.9326	0.9491
$\frac{1}{2}\tau_f + \frac{1}{2}\tau_f$	0.6892	0.8805	0.9325	0.9490

TABLE 3

NET FLUX $|\Delta F|$ IN SPECULAR REFLECTION

τ	$T = 20$, $B/A = 2$	τ	$T = 50$, $B/A = 5$
20.00	3.90×10^{-7}	50.00	1.40×10^{-7}
18.00	3.60×10^{-6}	45.00	1.90×10^{-6}
16.00	7.30×10^{-6}	40.00	4.22×10^{-6}
14.00	1.13×10^{-6}	35.00	7.30×10^{-6}
12.00	1.53×10^{-5}	30.00	1.17×10^{-6}
10.00	1.60×10^{-5}	25.00	1.58×10^{-5}
8.00	2.42×10^{-5}	20.00	2.12×10^{-4}
6.00	2.81×10^{-4}	15.00	2.73×10^{-4}
4.00	3.40×10^{-5}	10.00	3.43×10^{-5}
2.00	3.93×10^{-6}	5.00	2.23×10^{-5}
1.00	4.20×10^{-6}	2.50	4.66×10^{-5}
0.40	4.36×10^{-6}	1.00	4.92×10^{-5}
0.20	4.40×10^{-5}	0.50	5.01×10^{-4}
0.10	4.21×10^{-5}	0.25	5.03×10^{-5}
0.08	4.40×10^{-5}	0.20	5.04×10^{-4}
0.06	4.30×10^{-4}	0.15	5.03×10^{-5}
0.04	4.30×10^{-5}	0.10	5.02×10^{-5}
0.02	4.39×10^{-5}	0.05	5.01×10^{-5}

We calculate the net flux given by the formula

$$|\Delta F|_n = \left| \sum_{j=1}^{J} \mu_j C_j (U_n^+ - U_n^-) \right| = 0 \,, \tag{76}$$

where J is the number of angles and n is the shell number. From Table 3, we notice that the equation (76) is satisfied to the machine accuracy. This calculation shows that the flux is conserved at all points in the medium, which includes the global conservation of flux.

The method passed the above tests satisfactorily, and a numerical analysis of the method is under study. We are also applying this method in a polychromatic situation in an expanding envelope of a stellar atmosphere.

IV. CONCLUSIONS

We developed a numerical solution of the radiative transfer equation in spherically symmetric media by using integral operators. We have tested the method for the invariance of the specific intensity in vacuum, uniqueness, continuity, and stability of the numerical solution in a purely scattering medium. It has been successfully tested for a zero net flux condition at a totally reflecting surface.

The time taken for calculating the reflection, transmission matrices, and diffuse matrices in a fundamental shell is 0.02 s on the IBM 370/150 machine.

One of us (A. P.) would like to thank Dr. I. P. Grant of Pembroke College, Oxford, England, for directing his attention toward this kind of approach of solving the radiative transfer problems.

APPENDIX

The two pairs of transmission and reflection operators are given by

$$\begin{aligned} \boldsymbol{t}(i, i-1) &= \boldsymbol{R}^{+-}[\boldsymbol{\Delta}^{+}\boldsymbol{A} + \boldsymbol{r}^{+-}\boldsymbol{\Delta}^{-}\boldsymbol{C}] \,, \\ \boldsymbol{t}(i-1, i) &= \boldsymbol{R}^{-+}[\boldsymbol{\Delta}^{-}\boldsymbol{D} + \boldsymbol{r}^{-+}\boldsymbol{\Delta}^{+}\boldsymbol{B}] \,, \\ \boldsymbol{r}(i, i-1) &= \boldsymbol{R}^{-+}[\boldsymbol{\Delta}^{-}\boldsymbol{C} + \boldsymbol{r}^{-+}\boldsymbol{\Delta}^{+}\boldsymbol{A}] \,, \\ \boldsymbol{r}(i-1, i) &= \boldsymbol{R}^{+-}[\boldsymbol{\Delta}^{+}\boldsymbol{B} + \boldsymbol{r}^{+-}\boldsymbol{\Delta}^{-}\boldsymbol{D}] \,, \end{aligned} \tag{A1}$$

where

$$\boldsymbol{R}^{+-} = [\boldsymbol{I} - \boldsymbol{r}^{+-}\boldsymbol{r}^{-+}]^{-1} \,, \tag{A2}$$

$$\boldsymbol{\Sigma}^{+}_{i-1/2} = \tau_{i-1/2}(1 - \varpi)\boldsymbol{R}^{+-}[\boldsymbol{\Delta}^{+}\boldsymbol{B}^{+} + \boldsymbol{r}^{+-}\Delta^{-}\boldsymbol{B}^{-}] \,.$$

Similarly $\boldsymbol{R}^{-+}$ and $\boldsymbol{\Sigma}^{-}_{i-1/2}$ may be obtained by interchanging the plus and minus signs.

Further,

$$\begin{aligned} &\boldsymbol{\Delta}^{+} = [\boldsymbol{M}_1 - \bar{\boldsymbol{\rho}}_{+} + \tfrac{1}{2}\boldsymbol{\tau}^{+}(\boldsymbol{I} - \boldsymbol{\gamma}^{++})]^{-1} \,, \qquad \boldsymbol{\Delta}^{-} = [\boldsymbol{M}_4 + \bar{\boldsymbol{\rho}}_{-} + \tfrac{1}{2}\boldsymbol{\tau}^{-}(\boldsymbol{I} - \boldsymbol{\gamma}^{--})]^{-1} \,, \\ &\boldsymbol{A} = [\boldsymbol{M}_3 + \bar{\boldsymbol{\rho}}_{-} - \tfrac{1}{2}\boldsymbol{\tau}^{-}(\boldsymbol{I} - \boldsymbol{\gamma}^{++})] \,, \quad \boldsymbol{B} = \tfrac{1}{2}\boldsymbol{\tau}^{+}\boldsymbol{\gamma}^{+-} \,, \quad \boldsymbol{C} = \tfrac{1}{2}\boldsymbol{\tau}^{-}\boldsymbol{\gamma}^{-+} \,, \quad \boldsymbol{D} = [\boldsymbol{M}_2 - \bar{\boldsymbol{\rho}}_{+} - \tfrac{1}{2}\boldsymbol{\tau}^{+}(\boldsymbol{I} - \boldsymbol{\gamma}^{--})] \,, \\ &\boldsymbol{r}^{+-} = \tfrac{1}{2}\boldsymbol{\tau}^{-}\boldsymbol{\Delta}^{+}\boldsymbol{\gamma}^{+-} \,, \qquad \boldsymbol{r}^{-+} = \tfrac{1}{2}\boldsymbol{\tau}^{+}\boldsymbol{\Delta}^{-}\boldsymbol{\gamma}^{-+} \,. \end{aligned} \tag{A3}$$

REFERENCES

Abramowitz, M., and Stegun, I. 1970, *Handbook of Mathematical Functions* (New York: Dover).
Grant, I. P., and Hunt, G. E. 1969*a*, *Proc. Roy. Soc. London, A*, **313**, 183.
———. 1969*b*, *Proc. Roy. Soc. London, A*, **313**, 199.
Hummer, D. G., and Rybicki, G. B. 1971, *M.N.R.A.S.*, **152**, 1.
Kalkofen, W., and Wehrse, R. 1974, in *Methods in Radiative Transfer*, ed. W. Kalkofen (Cambridge: Cambridge University Press), p. 307.
Lathrop, K. D., and Carlson, B. G. 1967, *J. Comput. Phys.* **2**, 173.
———. 1971, *J. Quant. Spectrosc. Rad. Transf.*, **11**, 921.
Mihalas, D. 1978, *Stellar Atmospheres* (San Francisco: Freeman).
Peraiah, A. 1984, in *Methods in Radiative Transfer*, ed. W. Kalkofen (Cambridge: Cambridge University Press), p. 281.
Peraiah, A., and Grant, I. P. 1973, *J. Inst. Math. Appl.*, **12**, 75.
Preisendorfer, R. W. 1965, *Radiative Transfer on Discrete Spaces* (Pergamon: Oxford).
Schmid-Burgk, J. 1973, *Ap. J.*, **181**, 865.
———. 1975, *Astr. Ap.*, **40**, 249.

A. PERAIAH and B. A. VARGHESE: Indian Institute of Astrophysics, Bangalore 560034, India